Continuous-discrete multiple target tracking with out-of-sequence measurements

Ángel F. García-Fernández, Wei Yi

***Abstract*—This paper derives the optimal Bayesian processing of an out-of-sequence (OOS) set of measurements in continuous-time for multiple target tracking. We consider a multi-target system modelled in continuous time that is discretised at the time steps when we receive the measurements, which are distributed according to the standard point target model. All information about this system at the sampled time steps is provided by the posterior density on the set of all trajectories. This density can be computed via the continuous-discrete trajectory Poisson multi-Bernoulli mixture (TPMBM) filter. When we receive an OOS measurement, the optimal Bayesian processing performs a retrodiction step that adds trajectory information at the OOS measurement time stamp followed by an update step. After the OOS measurement update, the posterior remains in TPMBM form. We also provide a computationally lighter alternative based on a trajectory Poisson multi-Bernoulli filter. The effectiveness of the two approaches to handle OOS measurements is evaluated via simulations.**

***Index Terms*—Multiple target tracking, sets of trajectories, Poisson multi-Bernoulli mixtures, out-of-sequence measurements.**

I. Introduction

Multiple target tracking (MTT) systems are ubiquitous in many applications ranging from air-traffic control to driving assistance systems [1]–[3]. In MTT, there are an unknown number of targets that may appear, move and disappear from a scene of interest, and the objective is to infer their trajectories based on noisy sensor measurements.

In multi-sensor tracking systems, these measurements are usually obtained in scans and are sent to a processing center. Due to different time delays in transmission, a measurement scan may be received out-of-sequence (OOS). That is, the processing center has already processed some up-to-date information, and receives sensor information obtained at a past time. To use all available sensor information and improve tracking performance, it is of interest to process these OOS measurements in a computationally efficient manner, i.e., without having to reprocess previously received measurements [4].

Optimal algorithms to process an OOS measurement for a single target in linear Gaussian systems were provided in [5]–[7], and for nonlinear/non-Gaussian systems in [8]. Processing an OOS measurements can be done with a retrodiction step, which obtains target information at the time stamp of the OOS measurement, and a measurement update. This approach was extended in [4], [9], [10] to consider the posterior of a single trajectory, and in [11], to include multiple OOS measurements. OOS measurement processing algorithms for a fixed and known number of targets, or with external track initiation and termination, are provided in [12]–[14] and [15], [16], respectively. An approximate algorithm for processing OOS measurements within a probabilistic hypothesis density filter is provided in [17].

In this paper, we derive the exact Bayesian update with an OOS set of measurements, with a continuous-time time stamp, for multi-target systems. In this setting, at the OOS measurement time, we have to account for target appearances and disappearances in continuous time, including the possible existence of targets that did not exist at previously sampled time steps.

In order to explain the processing of an OOS measurement, we first review how to process the in-sequence measurements in a Bayesian manner. We consider a continuous-time multi-target system [18]–[20] in which target appearance and disappearance are given by an $\mathrm{M}/\mathrm{M}/\infty$ queuing system [21] and single-target dynamics are modelled by a stochastic differential equation (SDE) [22]. This multi-target system can be discretised at the time steps when we receive in-sequence measurements to obtain a standard multi-target dynamic model [23], which consists of a time-dependent probability of survival, single-target transition density and a Poisson point process (PPP) birth model [18].

All information on the set of all (sampled) trajectories, i.e., trajectories that have been discretised at the time steps when we receive the measurements, is contained in its posterior density [24]. For in-sequence measurements, the posterior is a Poisson multi-Bernoulli mixture (PMBM) that can be calculated by the trajectory Poisson multi-Bernoulli mixture (TPMBM) filter [25]–[27] with the resulting discretised multi-target dynamic model. The TPMBM filter is an extension of the PMBM filter [28], [29] for sets of targets to sets of trajectories. When the system is modelled in continuous time, we refer to the TPMBM filter as the continuous-discrete TPMBM (CD-TPMBM) filter. The TPMBM and PMBM filters are state-of-the-art multiple hypothesis tracking algorithms [30], with a Bayesian birth model and an efficient representation of the posterior via probabilistic target existence [28], [31], [32] and a PPP intensity to keep undetected target information, which is important, for example, in search-and-track operations [33].

The first contribution of this paper is that we derive the Bayesian processing of an OOS set of measurements in an MTT system by applying a retrodiction step followed

A. F. García-Fernández is with the Department of Electrical Engineering and Electronics, University of Liverpool, Liverpool L69 3GJ, United Kingdom, and also with the ARIES Research Centre, Universidad Antonio de Nebrija, Madrid, Spain (angel.garcia-fernandez@liverpool.ac.uk). Wei Yi is with the School of Information and Communication Engineering, the University of Electronic Science and Technology of China, China (kussoyi@gmail.com).

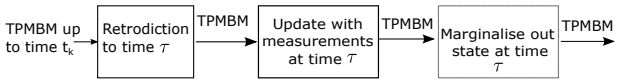

Figure 1: Diagram of the update with a set of OOS measurements at time τ. The posterior over the set of all (sampled) trajectories up to the current time step t_k is a PMBM. To process the OOS measurements, we perform a retrodiction step, which yields a PMBM density that includes trajectory information at time τ. The update of a TPMBM density results in another TPMBM density. We marginalise out the trajectory information at time τ to only keep trajectory information on the in-sequence sampled times, which yields a PMBM density.

by a measurement update. The retrodiction step takes into account continuous-time target appearances, dynamics and disappearances. This step adds state information at the OOS measurement time for the previously sampled trajectories and new trajectories that were not discretised at the in-sequence sampling times. Importantly, we show that the posterior keeps the PMBM form after the retrodiction and update steps. In order to only keep trajectory information at in-sequence sampling times, we then marginalise out trajectory information at OOS measurement time, which also keeps the PMBM form [34], see Figure 1.

The second contribution of this paper is to derive the Gaussian implementation of the OOS measurement processing when the SDE corresponds to the Wiener velocity model [22]. To enable a Gaussian implementation of the CD-TPMBM filter, we first obtain the best Gaussian PPP approximation to the birth model by minimising the Kullback-Leibler divergence (KLD) [18]. The resulting discretised model, along with linear/Gaussian measurement models with constant probability of detection, directly allows us to implement the CD-TPMBM filter in its Gaussian form [25], [27]. To carry out the OOS measurement processing for the Gaussian CD-TPMBM filter, we also require a KLD minimisation to account for new trajectories at the OOS time.

The obtained OOS measurement update can also be used with the continuous-discrete (track-oriented) trajectory Poisson multi-Bernoulli (CD-TPMB) filter, which is an approximation to the CD-TPMBM filter that only has one mixture component [27], [28], [35]. The (track-oriented) Poisson multi-Bernoulli filter is a variant of the joint integrated probabilistic data association filter [1] that accounts for the influence of undetected targets in the association events [28, Sec. IV.A]. Finally, we evaluate the benefits of OOS measurement processing for both the CD-TPMBM and CD-TPMB filters via simulations.

The rest of the paper is organised as follows. Section II provides an overview on the considered models. Section III explains the continuous-discrete models and the CD-TPMBM filter. The update of the CD-TPMBM filter with an OOS measurement is addressed in Section IV. Section V provides the Gaussian implementation of the OOS measurement update. Simulation results are provided in Section VI. Finally, conclusions are drawn in Section VII.

II. Background

This section provides a general background on the models used to solve the problem of continuous-discrete multiple target tracking with in-sequence measurements. The main notation of the paper is summarised in Table I.

Table I: Notation

- $\mathbf{x}_k$: set of targets at time step k, $x \in \mathbf{x}_k$ is a target state.
- $\mathbf{X}_k$: set of all sampled trajectories up to time step k.
- $X = \left(\beta, x^{1:\nu}\right) \in \mathbf{X}_k$: a trajectory state, with start time step β, length ν and states $\left(x^1, ..., x^\upsilon\right)$ (sampled at the in-sequence sampling times).
- $\mathbf{Y}_k$: set of all sampled trajectories up to time step k, including information at OOS time τ.
- $\left(u, \beta, x^{1:\nu}\right) \in \mathbf{Y}_k$: a trajectory with information at OOS time τ.
  - $u = 1$: trajectory exists at OOS time with state x^ν.
  - $u = 1$, $\beta = -1$, $\nu = 1$: OOS new trajectory (it was not sampled at the in-sequence sampling times, e.g. the blue one in Fig. 2).
  - $u = 0$: trajectory does not exist at OOS time.
- $f_{k|k'}(\cdot)$: density of $\mathbf{X}_k$ given measurements up to time step k'.
- $f_{\tau,k|k}(\cdot)$: density of $\mathbf{Y}_k$ given measurements up to time step k, but not at time τ.
- $f_{\tau,k|,\tau,k}(\cdot)$: density of $\mathbf{Y}_k$ given measurements up to time step k, including time τ.
- λ: rate of appearance of new targets.
- μ: rate of the exponentially distributed life span of a target.
- $g_{(\Delta t_k)}(\cdot\,|x)$: single target transition density from state x with a time interval Δt_k.

A. Sets of targets

The multi-target state at time t, where $t \in [0, \infty)$, is the set $\mathbf{x}(t) \in \mathcal{F}(\mathbb{R}^{n_x})$, where $\mathbb{R}^{n_x}$ is the single-target space, and $\mathcal{F}(\mathbb{R}^{n_x})$ is the space of all finite subsets of $\mathbb{R}^{n_x}$. Targets move independently with a continuous time model and, at any time t, targets may be added or removed from $\mathbf{x}(t)$. These models will be explained in Section III-A.

At time step $k \in \mathbb{N} \cup \{0\}$, which corresponds to a time t_k, we take noisy measurements from the multi-target state $\mathbf{x}_k = \mathbf{x}(t_k)$. These measurements are in-sequence, which means that $t_k > t_{k-1}$. At time step k, the set $\mathbf{z}_k \in \mathcal{F}(\mathbb{R}^{n_z})$ of measurements follows the standard point target measurement model [23]. That is, the set $\mathbf{z}_k$ is the union of the set of target-generated measurements and the set of clutter measurements. Given $\mathbf{x}_k$, each target $x \in \mathbf{x}_k$ is detected with probability $p^D(x)$ and generates a measurement with conditional density $l(\cdot|x)$, or missed with probability $1 - p^D(x)$. The clutter process is an independent PPP with intensity $\lambda^C(\cdot)$.

The posterior density of $\mathbf{x}_k$ given the sequence $\mathbf{z}_{1:k} = (\mathbf{z}_1, ..., \mathbf{z}_k)$ of measurements is a PMBM density that can be computed via the prediction and update equations with continuous-discrete dynamic models [18], [28], which will be explained in Section III-B.

B. Sets of sampled trajectories

In order to include target trajectory information in the filter, we consider target trajectories up to the current time t_k sampled at the times when the in-sequence measurements are taken. Specifically, a trajectory is characterised by its initial time step $\beta \in \{0, 1, ..., k\}$, its length υ (number of time steps that the trajectory has been present) and, its sequence $x^{1:\nu} = \left(x^1, ..., x^\upsilon\right)$ of target states from time step β to time step $\beta + \nu - 1$. A trajectory up to time step k is a variable $X = \left(\beta, x^{1:\nu}\right)$, where (β, ν) belongs to the set

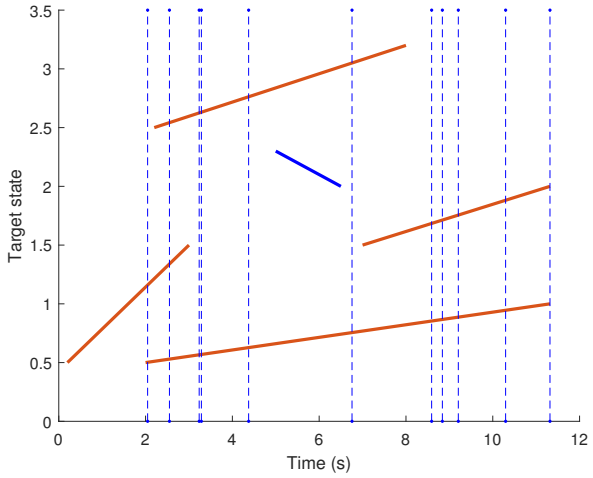

Figure 2: Illustration of a set of one-dimensional trajectories in continuous time and its discretisation. The vertical dashed lines indicate the times at which measurements have been taken, which are used to discretise the trajectories. The set $\mathbf{X}_k$ of sampled trajectories is shown in red (the trajectories exist at least at one of the sampled times). The blue trajectory has not been sampled and does not belong to $\mathbf{X}_k$.

$I_{(k)} = \{(\beta,\nu) : 0 \leq \beta \leq k \text{ and } 1 \leq \nu \leq k-\beta+1\}$, which ensures that the beginning and end of the trajectory belong to the considered time window. The single-trajectory space up to time step k is $T_{(k)} = \uplus_{(\beta,\nu)\in I_{(k)}} \{\beta\} \times \mathbb{R}^{\nu n_x}$, where $\uplus$ stands for disjoint union, which is used to highlight that the sets are disjoint. The set of (sampled) trajectories up to time step k is denoted by $\mathbf{X}_k \in \mathcal{F}\left(T_{(k)}\right)$.

Example 1. We consider one-dimensional targets and the five trajectories in continuous time shown in Figure 2. We have received measurements at the times indicated by the vertical dashed lines. The continuous trajectories are discretised at these time steps to obtain a set $\mathbf{X}_k$ of (sampled) trajectories. For example, the trajectory that appears first is (approximately) represented in discretised form as $(1, (1.16, 1.34))$. This means that it was born with the first round of measurements with a state 1.16, has a duration of two time steps, and has a state 1.34 at time step two. The discretised version of the rest of the trajectories is obtained analogously. The blue trajectory does not belong to $\mathbf{X}_k$, as it appeared and disappeared in between sampling times. These types of unobserved trajectories will play an important role in OOS measurement updates, see Section IV. $\diamondsuit$

Similarly to integrals on a single-target space $\mathbb{R}^{n_x}$, we can define integrals on the single-trajectory space $T_{(k)}$. For a real-valued function $\pi(\cdot)$ on the single-trajectory space, its integral is [24]

$$\int \pi(X)\, dX = \sum_{(\beta,\nu)\in I_{(k)}} \int \pi\left(\beta, x^{1:\nu}\right) dx^{1:\nu}. \tag{1}$$

This integral sums over all possible start times and lengths, and integrates the sequence of states. Integral (1) is the basis for the set integral on trajectories [24].

III. Continuous-discrete trajectory PMBM filter

This section describes the CD-TPMBM filter for in-sequence measurements. Before this, Sections III-A and III-B review the continuous and continuous-discrete multi-target models.

Following [18], we use the terms target appearance and disappearance for the continuous time process, and target birth and death for the discretised process. A target appearance may not imply target birth, as the target may appear and disappear in between two sampling times, see Figure 2.

A. Continuous time multi-target model

The continuous time multi-target model has the following characteristics [18]. A Poisson process (in time) with rate λ models the times of target appearances [21]. The life span of a target is independent and exponentially distributed with rate μ. These two properties define an $\mathrm{M}/\mathrm{M}/\infty$ queuing system [21] for the evolution of the number of targets across time.

The distribution of a target state at the time of appearance is an independent Gaussian with mean $\overline{x}_a$ and covariance matrix P_a. Targets move independently following an SDE [22]

$$dx(t) = Ax(t)\, dt + L d\varpi(t) \tag{2}$$

where $x(t) \in \mathbb{R}^{n_x}$ is the target state at time t, $A \in \mathbb{R}^{n_x \times n_x}$ and $L \in \mathbb{R}^{n_x \times n_\beta}$ are matrices, $dx(t)$ is the differential of $x(t)$, and $\varpi(t) \in \mathbb{R}^{n_\varpi}$ is a Brownian motion with diffusion matrix Q_ϖ.

B. Continuous-discrete multi-target model

The continuous time model in Section III-A is discretised at the times when we receive in-sequence measurements. The resulting discretised model results in a (time-dependent) standard multi-target dynamic model [23], in which targets evolve independently and target birth is also independent. In particular, given $\mathbf{x}_{k-1}$, each $x \in \mathbf{x}_{k-1}$ survives to time step k with a probability of survival

$$p_k^S = e^{-\mu \Delta t_k}, \tag{3}$$

where $\Delta t_k = t_k - t_{k-1}$, and moves to a new state with transition density $g_{(\Delta t_k)}(\cdot\,|x)$ [22]

$$g_{(\Delta t_k)}\left(x(t_k)\,|x(t_{k-1})\right) = \mathcal{N}\left(x(t_k); F_{(\Delta t_k)} x(t_{k-1}), Q_{(\Delta t_k)}\right) \tag{4}$$

$$F_{(\Delta t_k)} = \exp\left(A \Delta t_k\right) \tag{5}$$

$$Q_{(\Delta t_k)} = \int_0^{\Delta t_k} \exp\left(A\left(\Delta t_k - \xi\right)\right) L Q_\varpi L^T \times \exp\left(A\left(\Delta t_k - \xi\right)\right)^T d\xi \tag{6}$$

where superscript T denotes transpose, $\exp(A)$ denotes the matrix exponential of A and $\mathcal{N}(x; \overline{x}, Q)$ denotes a Gaussian density with mean $\overline{x}$ and covariance matrix Q evaluated at x.

Targets are born according to a PPP with intensity

$$\lambda_k^B(x_k) = \frac{\lambda}{\mu}\left(1 - e^{-\mu \Delta t_k}\right) \int_0^{\Delta t_k} p\left(x_k\,|t\right) p_{(\Delta t_k)}(t)\, dt \tag{7}$$

$$p\left(x_k\left|t\right.\right)=\mathcal{N}\left(x_k;F_{(t)}\overline{x}_a,F_{(t)}P_aF_{(t)}^T+Q_{(t)}\right) \tag{8}$$

$$p_{(\Delta t_k)}\left(t\right)=\frac{\mu}{1-e^{-\mu\Delta t_k}}e^{-\mu t}\chi_{[0,\Delta t_k)}\left(t\right) \tag{9}$$

where $\chi_{[0,\Delta t_k)}\left(t\right)=1$ if $t\in[0,\Delta t_k)$ and $\chi_{[0,\Delta t_k)}\left(t\right)=0$ otherwise. The quantity $\frac{\lambda}{\mu}\left(1-e^{-\mu\Delta t_k}\right)$ is the expected number of targets that are born at time step k, i.e., targets that appeared between times t_{k-1} and t_k and are still alive at time t_k [18], [36]. For example, the blue trajectory in Figure 2 is not considered in the birth model as it has not been sampled. Eq. (9) is a truncated exponential density with parameter μ in the interval $[0,\Delta t_k)$ and represents the density of the time lag t of new born targets. That is, if a target appears at time step t_k-t with $t\in[0,\Delta t_k)$, then t denotes the time lag between appearing time and t_k. Density (8) represents the single-target density at time step t_k given that the target appeared with a time lag t.

C. CD-TPMBM filter

As the discretised dynamic model in Section III-B is a standard multi-target dynamic model, the posterior and predicted densities on the set of all trajectories (which include alive and dead trajectories) are PMBMs [25], [27].

Given $\mathbf{z}_{1:k'}$ with $k'\in\{k-1,k\}$, the density $f_{k|k'}\left(\cdot\right)$ of the set $\mathbf{X}_k$ of all trajectories up to the current time step k is a PMBM [25]–[27], [37]

$$f_{k|k'}\left(\mathbf{X}_k\right)=\sum_{\mathbf{X}^{\mathrm{u}}\uplus\mathbf{X}^{\mathrm{d}}=\mathbf{X}_k}f_{k|k'}^{\mathrm{p}}\left(\mathbf{X}^{\mathrm{u}}\right)f_{k|k'}^{\mathrm{mbm}}\left(\mathbf{X}^{\mathrm{d}}\right) \tag{10}$$

$$f_{k|k'}^{\mathrm{p}}\left(\mathbf{X}^{\mathrm{u}}\right)=e^{-\int\lambda_{k|k'}(X)dX}\prod_{X\in\mathbf{X}^{\mathrm{u}}}\lambda_{k|k'}\left(X\right) \tag{11}$$

$$f_{k|k'}^{\mathrm{mbm}}\left(\mathbf{X}^{\mathrm{d}}\right)=\sum_{a\in\mathcal{A}_{k|k'}}w_{k|k'}^{a}\sum_{\uplus_{l=1}^{n_{k|k'}}\mathbf{X}^l=\mathbf{X}^{\mathrm{d}}}\prod_{i=1}^{n_{k|k'}}f_{k|k'}^{i,a^i}\left(\mathbf{X}^i\right) \tag{12}$$

where in (10) we sum over all disjoint and possibly empty sets $\mathbf{X}^{\mathrm{u}}$ and $\mathbf{X}^{\mathrm{d}}$ such that $\mathbf{X}^{\mathrm{u}}\cup\mathbf{X}^{\mathrm{d}}=\mathbf{X}_k$, and

$$f_{k|k'}^{i,a^i}\left(\mathbf{X}\right)=\begin{cases}1-r_{k|k'}^{i,a^i} & \mathbf{X}=\emptyset\\ r_{k|k'}^{i,a^i}p_{k|k'}^{i,a^i}\left(X\right) & \mathbf{X}=\{X\}\\ 0 & \text{otherwise.}\end{cases} \tag{13}$$

We proceed to describe the aspects of (10) that are relevant to this work. Details can be found in [25]. The density $f_{k|k'}\left(\cdot\right)$ is the union of two independent random finite sets: a PPP with density $f_{k|k'}^{\mathrm{p}}\left(\cdot\right)$ and intensity $\lambda_{k|k'}\left(\cdot\right)$, and a multi-Bernoulli mixture (MBM) with density $f_{k|k'}^{\mathrm{mbm}}\left(\cdot\right)$. The PPP contains information on trajectories that have never been detected, but have been discretised at in-sequence measurements, see Figure 2. The number of potential trajectories that have ever been present and detected in the surveillance area is $n_{k|k'}$, which is the number of Bernoullis in each MBM component. Each received measurement generates one of these potential trajectories, which are indexed by i. A global hypothesis is $a=\left(a^1,...,a^{n_{k|k'}}\right)$, where $a^i\in\left\{1,...,h^i\right\}$ is the index to the local hypothesis for the i-th potential trajectory and h^i is the number of local hypotheses. Each global hypothesis corresponds to a multi-Bernoulli in the MBM, and indicates a possible way to associate the received measurements so far to potential trajectories. The density of the i-th potential trajectory with local hypothesis a^i is Bernoulli $f_{k|k'}^{i,a^i}\left(\cdot\right)$, whose probability of existence is $r_{k|k'}^{i,a^i}$ and its single-trajectory density is $p_{k|k'}^{i,a^i}\left(\cdot\right)$. The set of all global hypotheses is $\mathcal{A}_{k|k'}$ [28].

The TPMBM posterior (10) can be calculated recursively via a prediction and an update step [25], [37]. The prediction step is performed as in the TPMBM filter using the corresponding (interval dependent) probability of survival, single-target transition density and intensity of new born targets, see (3), (4) and (7). The update step is similar to the TPMBM filter update.

IV. CD-TPMBM update with OOS measurements

This section explains the Bayesian processing of OOS measurements based on the posterior (10). Section IV-A defines the retrodicted set of trajectories. Section IV-B and IV-C explain the retrodiction and update steps. Section IV-D addresses the marginalisation step.

A. Retrodicted set of trajectories

We consider we know the PMBM posterior over the set $\mathbf{X}_k$ of all (sampled) trajectories up to the current time t_k, $f_{k|k}\left(\cdot\right)$ in (10). We receive an OOS set of measurements with time stamp τ, such that $t_0<\tau<t_k$. The closest previously sampled time steps to τ are k^o-1 and k^o, with continuous times $t_{k^o-1}<\tau$ and $t_{k^o}>\tau$. We denote $\Delta t_{o,1}=\tau-t_{k^o-1}$ and $\Delta t_{o,2}=t_{k^o}-\tau$.

To perform the update with this OOS set of measurements, we first perform a retrodiction step in which we calculate the density of the retrodicted set $\mathbf{Y}_k$ of trajectories, e.g., the set of all trajectories including trajectory state information at time τ. The set $\mathbf{Y}_k$ can be written as $\mathbf{Y}_k=\mathbf{X}_k^{\mathrm{a}}\cup\mathbf{N}$, where $\mathbf{X}_k^{\mathrm{a}}$ corresponds to the set $\mathbf{X}_k$ with additional state information at time τ, and $\mathbf{N}$ denotes the set of trajectories that existed at time step τ, and appeared and disappeared between time steps k^o-1 and k^o. The trajectories in $\mathbf{N}$ do not belong to $\mathbf{X}_k$, see Figure 2, and we refer to them as OOS new trajectories at time τ.

We denote the retrodicted trajectories as $(u,Y)\in\mathbf{Y}_k$, where mark $u=0$ if the trajectory $Y=\left(\beta,x^{1:\nu}\right)$ does not exist at time τ (but exists at other sampled times) and $u=1$ if $Y=\left(\beta,x^{1:\nu}\right)$ exists at time τ, being the last state x^ν its state at time τ. More information on marks and point processes can be found at [38, Chap.8].

For notational convenience, we write $\left(u,\left(\beta,x^{1:\nu}\right)\right)=\left(u,\beta,x^{1:\nu}\right)$. In particular, if the trajectory $\left(\beta,x^{1:\nu}\right)\in\mathbf{X}_k$ does not exist at time τ, it is included in $\mathbf{X}_k^{\mathrm{a}}$ as $\left(0,\beta,x^{1:\nu}\right)$. If the trajectory $\left(\beta,x^{1:\nu}\right)\in\mathbf{X}_k$ exists at time τ, it is included in $\mathbf{X}_k^{\mathrm{a}}$ as $\left(1,\beta,x^{1:\nu},y\right)$, where its last state y is the state at time τ. These two possibilities are modelled by a transition density $g_{\tau,k|k}\left(\cdot|X\right)$ that converts each trajectory $X\in\mathbf{X}_k$ into $(u,Y)\in\mathbf{X}_k^{\mathrm{a}}$. As we explain in Section IV-B, the set $\mathbf{N}$ is a PPP independent of $\mathbf{X}_k^{\mathrm{a}}$ and a trajectory $(u,Y)\in\mathbf{N}$ is represented as $(1,\beta,x)$, where we set $u=1$ and $\beta=-1$ to

mark that it is an OOS new trajectory. We proceed to illustrate with an example how sets $\mathbf{X}_k^{\mathrm{a}}$ and $\mathbf{N}$ are formed.

Example 2. Let us consider we have the trajectories in Example 1 and Figure 2. We receive an OOS measurement at time $\tau = 6\,\mathrm{s}$. The trajectory that appeared first $(1,(1.16,1.34)) \in \mathbf{X}_k$ does not exist at τ so it in included in $\mathbf{X}_k^{\mathrm{a}}$ as $(0,1,(1.16,1.34))$. The trajectory on top in Figure 2, $(2,(2.55,2.63,2.63,2.76,3.05)) \in \mathbf{X}_k$ exists at τ so it is included in $\mathbf{X}_k^{a}$ as $(1,2,(2.55,2.63,2.63,2.76,3.05,2,96))$, where 2.96 is the trajectory state at τ. The blue trajectory was not previously sampled and exists at τ, so it belongs to $\mathbf{N}$ and has a state $(1,-1,2.1)$. $\diamondsuit$

The single retrodicted trajectory space is then

$$\uplus_{u=0}^{1} \uplus_{(\beta,\nu)\in I_{(k,u)}} \{u\} \times \{\beta\} \times \mathbb{R}^{\nu n_x},$$

where $I_{(k,0)} = I_{(k)}$ and $I_{(k,1)} = \{(-1,1)\} \cup \{(\beta,\nu) : 0 \leq \beta \leq k \,\text{and}\, 1 \leq \nu \leq k-\beta+2\}$. For a real-valued function $\pi(\cdot)$ on the single-retrodicted space, its integral is

$$\int \pi(u,Y)\, d(u,Y) = \sum_{u=0}^{1} \sum_{(\beta,\nu)\in I_{(k,u)}} \int \pi\left(u,\beta,x^{1:\nu}\right) dx^{1:\nu}. \tag{14}$$

B. Retrodiction step

Given a trajectory $Y = \left(\beta, x^{1:\nu}\right)$, $\nu > 1$, the trajectory without the last state is denoted by $Y^{-} = \left(\beta, x^{1:\nu-1}\right)$. We also use symbols $\wedge$ and $\vee$ to denote "and" and "or", respectively. The transition density to obtain $(u,Y) \in \mathbf{X}_k^{\mathrm{a}}$ from $X \in \mathbf{X}_k$ is provided in the following proposition.

Proposition 3. *The transition density $g_{\tau,k|k}(\cdot|X)$ to augment each trajectory $X = \left(\beta, x^{1:\nu}\right) \in \mathbf{X}_k$ with state information at OOS time τ and produce $(u,Y) \in \mathbf{X}_k^{\mathrm{a}}$ is*

$$g_{\tau,k|k}(u,Y|X) = \begin{cases} \delta_X(Y)\,\delta_0[u] & \beta > k^o \vee \omega < k^o - 1 \\ \delta_X(Y^-) & \\ \times p\left(y|x^{k^o-\beta}, x^{k^o-\beta+1}\right)\delta_1[u] & \beta \leq k^o-1 \wedge \omega \geq k^o \\ \left(1-p_1^{S,o}\right)\delta_X(Y)\,\delta_0[u] + p_1^{S,o} & \\ \times \delta_X(Y^-)\, g_{(\Delta t_{o,1})}\left(y|x^{\nu}\right)\delta_1[u] & \omega = k^o - 1 \\ \left(1-p_2^{S,o}\right)\delta_X(Y)\,\delta_0[u] & \\ + p_2^{S,o}\delta_X(Y^-)\, p\left(y|x^1\right)\delta_1[u] & \beta = k^o \end{cases} \tag{15}$$

where y is the last state of Y, $\omega = \beta + \nu - 1$, $p_1^{S,o} = p_k^{S,o}(\Delta t_{o,1})$, $p_2^{S,o} = p_k^{S,o}(\Delta t_{o,2})$ with

$$p_k^{S,o}(\Delta t) = \frac{e^{-\mu\Delta t} - e^{-\mu\Delta t_{k^o}}}{1 - e^{-\mu\Delta t_{k^o}}} \tag{16}$$

and

$$p\left(y|x^{k^o-\beta}, x^{k^o-\beta+1}\right) = \frac{g_{(\Delta t_{o,2})}\left(x^{k^o-\beta+1}|y\right) g_{(\Delta t_{o,1})}\left(y|x^{k^o-\beta}\right)}{g_{(\Delta t_{k^o})}\left(x^{k^o-\beta+1}|x^{k^o-\beta}\right)} \tag{17}$$

$$p\left(y|x^1\right) = \frac{g_{(\Delta t_{o,2})}\left(x^1|y\right)\int_0^{\Delta t_{o,1}} p\left(y\,|t\right) p_{(\Delta t_{o,1})}(t)\, dt}{\int g_{(\Delta t_{o,2})}\left(x^1|y\right)\int_0^{\Delta t_{o,1}} p\left(y\,|t\right) p_{(\Delta t_{o,1})}(t)\, dt dy}. \tag{18}$$

The first entry in (15) indicates that if a trajectory X was born after k^o or its final time step ω occurred before k^o-1, its state does not exist at time τ with with probability one. That is, this entry considers trajectories that do not exist at time τ but exist at other sampled time steps. The second entry in (15) indicates that if a trajectory X was born at time step k^o-1, or earlier, and finished at time step k^o, or afterwards, then the trajectory exists at time τ with probability one. In addition, given the states of X at time steps k^o-1 and k^o, its state at at time τ can be directly obtained using Bayes' rule and the properties of the discretised single-target transition density (4), resulting in (17). The third entry in (15) considers a trajectory X that finished at time step k^o-1. This trajectory disappeared (in continuous time) at any time between t_{k^o-1} and t_{k^o}, and the probability that it disappeared between times τ and t_{k^o}, which implies that it existed at time τ, is $p_1^{S,o}$. If it exists, its state is obtained using the single-target transition density (4) with a time interval $\Delta t_{o,1}$. The fourth entry in (15) considers a trajectory X that was born at time step k^o. This trajectory appeared (in continuous time) at any time between t_{k^o-1} and t_{k^o}, and the probability that it appeared between times t_{k^o-1} and τ, which implies that it existed at time τ, is $p_2^{S,o}$. If it exist, its state at τ is given by applying Bayes' rule to its prior density at time step τ corrected by the information provided by its state at time t_{k^o}. The resulting transition density is (18). More details on how to calculate $p_1^{S,o}$ and $p_2^{S,o}$ are provided in Appendix A.

Once we have the transition density for the retrodiction step, we can obtain the PMBM retrodiction step via the following theorem.

Theorem 4. *Given the PMBM posterior $f_{k|k}(\cdot)$ in (10) on the set of all sampled trajectories, the retrodicted density on the set $\mathbf{Y}_k$ of trajectories augmented with information at time $\tau < t_k$ is a PMBM with density*

$$f_{\tau,k|k}(\mathbf{Y}_k) = \sum_{\mathbf{Y}^{\mathrm{u}}\uplus\mathbf{Y}^{\mathrm{d}}=\mathbf{Y}_k} f_{\tau,k|k}^{\mathrm{p}}\left(\mathbf{Y}^{\mathrm{u}}\right) f_{\tau,k|k}^{\mathrm{mbm}}\left(\mathbf{Y}^{\mathrm{d}}\right) \tag{19}$$

$$f_{\tau,k|k}^{\mathrm{p}}\left(\mathbf{Y}^{\mathrm{u}}\right) = e^{-\int \lambda_{\tau,k|k}(u,Y)d(u,Y)} \prod_{(u,Y)\in\mathbf{Y}^{\mathrm{u}}} \lambda_{\tau,k|k}(u,Y) \tag{20}$$

$$f_{\tau,k|k}^{\mathrm{mbm}}\left(\mathbf{Y}^{\mathrm{d}}\right) = \sum_{a\in\mathcal{A}_{k|k}} w_{k|k}^{a} \sum_{\uplus_{l=1}^{n_{k|k}}\mathbf{Y}^{l}=\mathbf{Y}^{\mathrm{d}}} \prod_{i=1}^{n_{k|k}} f_{\tau,k|k}^{i,a^i}\left(\mathbf{Y}^{i}\right) \tag{21}$$

where the intensity of the PPP $f_{\tau,k|k}^{\mathrm{p}}(\cdot)$ is

$$\lambda_{\tau,k|k}(u,Y) = \lambda_{\tau,k|k}^{B}(u,Y) + \int g_{\tau,k|k}(u,Y|X)\,\lambda_{k|k}(X)\, dX, \tag{22}$$

and the intensity of OOS new trajectories is

$$\lambda_{\tau,k|k}^{B}\left(u,\beta,x^{1:\nu}\right) = w^{B}(\Delta t_{o,1},\Delta t_{o,2})\,\delta_1[u]\,\delta_{-1}[\beta] \times \delta_1[\nu]\int_0^{\Delta t_{o,1}} p\left(x^1\,|t\right) p_{(\Delta t_{o,1})}(t)\, dt. \tag{23}$$

$$w^B\left(\Delta t_{o,1},\Delta t_{o,2}\right)=\frac{\lambda}{\mu}\left(1-e^{-\mu\Delta t_{o,1}}\right)\left(1-e^{-\mu\Delta t_{o,2}}\right). \tag{24}$$

The probability of existence and single-target density of Bernoulli $f^{i,a^i}_{\tau,k|k}\left(\cdot\right)$ *are*

$$r^{i,a^i}_{\tau,k|k}=r^{i,a^i}_{k|k} \tag{25}$$

$$p^{i,a^i}_{\tau,k|k}\left(u,Y\right)=\int g_{\tau,k|k}\left(u,Y|X\right)p^{i,a^i}_{k|k}\left(X\right)dX. \tag{26}$$

Theorem 4 is proved in Appendix A, and results from the application of the single-trajectory transition density in (3) to a PMBM density (10), accounting for the distribution of the set $\mathbf{N}$ of OOS new trajectories, which is a PPP with intensity $\lambda^B_{\tau,k|k}\left(\cdot\right)$.

The probability of existence of the Bernoulli components does not change, see (25). The reason is that all the trajectories that belong to $\mathbf{X}_k$ also belong to $\mathbf{Y}_k$, so there is no change in their probability of existence. A similar phenomenon happens in the TPMBM prediction step when we consider all trajectories [25], [27]. The single-target densities (26) are transformed using the transition density $g_{\tau,k|k}\left(\cdot|\cdot\right)$, which augments trajectories with state information at time τ. The intensity of the PPP (22) is the sum of the intensity $\lambda^B_{\tau,k|k}\left(\cdot\right)$ and the intensity of the undetected trajectories in $\mathbf{X}_k$ augmented with information at time τ. Equation (24) represents the expected number of OOS new trajectories. This number is the expected number of trajectories that appear in an interval $\Delta t_{o,1}$ and are alive at its end, which is given by $\frac{\lambda}{\mu}\left(1-e^{-\mu\Delta t_{o,1}}\right)$ [18], [36], multiplied by the probability that a trajectory disappears in an interval $\Delta t_{o,2}$, which is given by $\left(1-e^{-\mu\Delta t_{o,2}}\right)$, see (3).

We plot the mean number of OOS new trajectories, see (24), as a function of $\Delta t_{o,1}$ in one illustrative example in Figure 3. The maximum is obtained at the middle of the interval $\Delta t_{o,1}=\Delta t_{k^o}/2$, which can also be proved analytically. This means that if the OOS measurement falls in the middle of two sampled times, the number of OOS new trajectories is at its maximum. The mean number of OOS new trajectories increases with λ, as more targets appear in the scene. In addition, the mean number of OOS new trajectories initially increases with μ, but it then decreases. We recall that $1/\mu$ is the expected life span of the trajectories [18, Sec. II]. For sufficiently small μ, targets that appeared between t_{k^o-1} and τ are still alive at t_{k^o} with high probability and $w^B\left(\cdot\right)$ is small. As μ starts increasing, the probability that these targets are not alive at t_{k^o} increases, and therefore, $w^B\left(\cdot\right)$ increases. However, as μ increases the number of targets that appear between t_{k^o-1} and τ and are alive at τ also decreases, which implies that $w^B\left(\cdot\right)$ starts to decrease after a certain point.

C. Update step

The measurement model at time τ, see Section II-A, can be written in terms of $\mathbf{Y}_k$, as follows. Each trajectory $\left(u,\beta,x^{1:\nu}\right)\in\mathbf{Y}_k$ is detected with probability

$$p^D\left(u,\beta,x^{1:\nu}\right)=\begin{cases}p^D\left(x^\nu\right) & u=1\\ 0 & \text{otherwise}\end{cases} \tag{27}$$

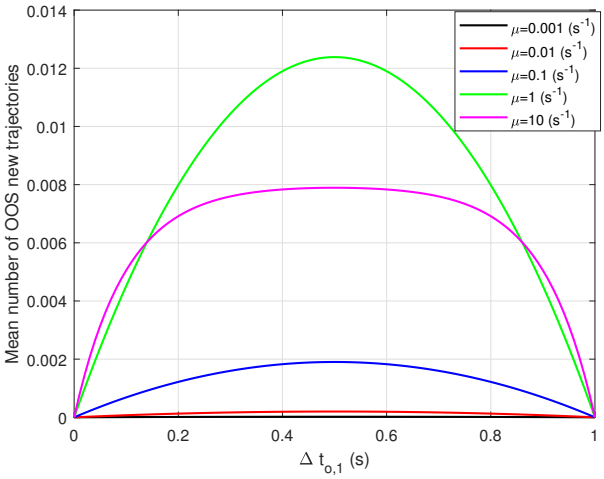

Figure 3: Mean number of OOS new trajectories, see (24), as a function of $\Delta t_{o,1}$ for a time interval $t_{k^o}-t_{k^o-1}=1\,\text{s}$ and $\lambda=0.08\,\text{s}^{-1}$. The maximum is achieved for the middle of the time interval $\Delta t_{o,1}=0.5\,\text{s}$.

and generates a measurement with density $l\left(\cdot|u,\beta,x^{1:\nu}\right)=l\left(\cdot|x^\nu\right)$, or misdetected with probability $1-p^D\left(u,\beta,x^{1:\nu}\right)$. The clutter model remains unchanged.

For this measurement model and a PMBM prior (19), the updated density $f_{\tau,k|,\tau,k}\left(\cdot\right)$ is also PMBM [25], [27], [28]. The update is analogous to the trajectory PMBM filter update [25], [27], but using the retrodicted trajectory integral (14).

D. Marginalisation

The steps in Sections IV-B and IV-C provide the closed-form update when we receive the first OOS set of measurements. In order to continue with the filtering recursion, we can proceed in two forms. One is to transform the augmented trajectories $\left(u,Y\right)$ into trajectories of the type $\left(\beta,x^{1:\nu}\right)$, with the states arranged in consecutive time steps. In order to do this, the time index k of the measurements changes as we insert a new measurement in the previous sequence. In addition, the meaning of β changes. For trajectories born the time step corresponding to τ, it represents trajectories in $\mathbf{N}$, which appear and disappear in between the two closest sampling times. If we follow this approach, it is possible to generalise the process in this section to deal with OOS measurements in an exact way.

However, as most of the measurements are expected to be in-sequence, we pursue the simpler approach of marginalising out the information at time τ. That is, once we have updated all trajectory information based on the OOS measurement, we only keep the information at the in-sequence measurement sampled times, not at OOS measurement times. This marginalisation can be obtained by applying the transition density

$$g_m\left(\mathbf{X}|\left(u,\beta,x^{1:\nu}\right)\right)=\begin{cases}\delta_\emptyset\left(\mathbf{X}\right) & \beta=-1\\ \delta_{\{(\beta,x^{1:\nu})\}}\left(\mathbf{X}\right) & \beta>-1,u=0\\ \delta_{\{(\beta,x^{1:\nu-1})\}}\left(\mathbf{X}\right) & \beta>-1,u=1\\ 0 & \text{otherwise}\end{cases} \tag{28}$$

to each trajectory in $\mathbf{Y}_k$. This transition density is actually a Bernoulli transition density with state dependent probability of survival. When applied to the updated PMBM, the result is a PMBM that discards trajectory information at time τ [26], [34].

Every time we receive an OOS measurement, we perform the steps of retrodiction, update and marginalisation. The procedure provides the exact solution posterior at the in-sequence sampling times unless we get more than one OOS set of measurements in the same time interval (t_{k^o-1}, t_{k^o}). In this case, the procedure is an approximation as, for the exact retrodiction in Theorem 4, we require access to the two closest states of the trajectories at the time steps when we have received measurements.

V. OOS MEASUREMENT PROCESSING WITH GAUSSIAN CD-TPMBM IMPLEMENTATION

This section explains how to process OOS measurements with a Gaussian implementation of the CD-TPMBM filter. The single-target models are explained in Section V-A, the Gaussian TPMBM posterior in Section V-B, the retrodiction step in Section V-C. Finally, practical aspects are discussed in Section V-D.

A. Single-target models

For the Gaussian implementation, we use a linear/Gaussian measurement model $l(\cdot|x) = \mathcal{N}(\cdot; Hx, R)$ and a constant probability p_D of detection. We consider the Wiener velocity model [22] for single-target dynamics with a single-target state

$$x(t_k) = [p_1(t_k), ..., p_d(t_k), v_1(t_k), ..., v_d(t_k)]^T \tag{29}$$

where $d = n_x/2$ is the dimension of the space where the target moves. For this dynamic model, we can obtain a best Gaussian fit to the PPP of new born targets that enables Gaussian implementations [18, Prop. 2]. This result directly extends to the PPP of OOS new trajectories in (23).

For the Wiener velocity model, we also have [22]

$$F_{(\Delta t_k)} = \begin{pmatrix} I_d & \Delta t_k I_d \\ 0_d & I_d \end{pmatrix} \tag{30}$$

$$Q_{(\Delta t_k)} = q \begin{pmatrix} \frac{(\Delta t_k)^3}{3} I_d & \frac{(\Delta t_k)^2}{2} I_d \\ \frac{(\Delta t_k)^2}{2} I_d & \Delta t_k I_d \end{pmatrix} \tag{31}$$

where q is a model parameter.

B. Gaussian TPMBM posterior

For the models explained in Section V-A, we can use the Gaussian implementation of the TPMBM filter for the set of all trajectories in [27]. We proceed to describe the main aspects. Details can be found in [25], [27].

A Gaussian density in the single-trajectory space is

$$\mathcal{N}\left(\beta, x^{1:\nu}; \overline{\beta}, \overline{x}, P\right) = \begin{cases} \mathcal{N}\left(x^{1:\nu}; \overline{x}, P\right) & \beta = \overline{\beta},\ \nu = \iota \\ 0 & \text{otherwise} \end{cases} \tag{32}$$

where $\iota = \dim(\overline{x})/n_x$ and $\dim(\overline{x})$ is the dimension of $\overline{x}$. Equation (32) represents a Gaussian trajectory density with start time $\overline{\beta}$, duration ι, mean $\overline{x} \in \mathbb{R}^{\iota n_x}$ and covariance matrix $P \in \mathbb{R}^{\iota n_x \times \iota n_x}$ evaluated at $\left(\beta, x^{1:\nu}\right)$.

The i-th Bernoulli component with local hypothesis a^i has a single-trajectory density

$$p_{k|k}^{i,a^i}(X) = \sum_{\kappa=\beta^{i,a^i}}^{k} \alpha_{k|k}^{i,a^i}(\kappa)\, \mathcal{N}\left(X; \beta^{i,a^i}, \overline{x}_{k|k}^{i,a^i}(\kappa), P_{k|k}^{i,a^i}(\kappa)\right) \tag{33}$$

where β^{i,a^i} is the start time, $\alpha_{k|k}^{i,a^i}(\kappa)$ is the probability that the corresponding trajectory terminates at time step κ (conditioned on existence), and $\overline{x}_{k|k}^{i,a^i}(\kappa) \in \mathbb{R}^{\iota n_x}$ and $P_{k|k}^{i,a^i}(\kappa) \in \mathbb{R}^{\iota n_x \times \iota n_x}$, with $\iota = \kappa - \beta^{i,a^i} + 1$, are the mean and the covariance matrix of the trajectory given that it ends at time step κ. The coefficients $\alpha_{k|k}^{i,a^i}(\kappa)$, $\kappa = \beta^{i,a^i}, ..., k$, sum to one.

For simplicity, the intensity of the PPP only considers alive trajectories and has the form

$$\lambda_{k|k}(X) = \sum_{q=1}^{n_{k|k}^p} w_{k|k}^{p,q} \mathcal{N}\left(X; \beta_{k|k}^{p,q}, \overline{x}_{k|k}^{p,q}, P_{k|k}^{p,q}\right) \tag{34}$$

where $n_{k|k}^p$ is the number of components, $w_{k|k}^{p,q}$, $\beta_{k|k}^{p,q}$, $\overline{x}_{k|k}^{p,q}$ and $P_{k|k}^{p,q}$ are the weight, starting time, mean and covariance matrix of the qth component, respectively. As the PPP trajectories are alive, $\beta_{k|k}^{p,q} + \dim\left(\overline{x}_{k|k}^{p,q}\right)/n_x - 1 = k$.

C. OOS retrodiction step

To perform the retrodiction step, we need to calculate (22) and (26) when the input is (33) and (34). These results can be directly established by calculating the integral (26) for a Gaussian input (32). We denote $F_1 = F_{(\Delta t_{o,1})}$, $F_2 = F_{(\Delta t_{o,2})}$, $Q_1 = Q_{(\Delta t_{o,1})}$ and $Q_2 = Q_{(\Delta t_{o,2})}$.

We approximate the integral w.r.t. time in (18) for the Wiener velocity model by its best Gaussian fit via KLD minimisation. The resulting moments, called $\overline{x}_{b,1}$ and $P_{b,1}$, are given by Prop. 2 in [18] using $\Delta t_{o,1}$ as the time interval. The rest of the calculations are closed-form to yield this lemma.

Lemma 5. *Given $p(X) = \mathcal{N}\left(X; \overline{\beta}, \overline{x}, P\right)$ and $g_{\tau,k|k}(\cdot|X)$ in Prop. 3 and the best Gaussian fit to the integral in (18), with moments $\overline{x}_{b,1}$ and $P_{b,1}$ [18, Prop. 2], the density of its augmented trajectory (u, Y) is*

$$\int g_{\tau,k|k}(u, Y|X)\, p(X)\, dX = \begin{cases} p(Y)\, \delta_0[u] & \overline{\beta} > k^o \vee \omega < k^o - 1 \\ \mathcal{N}\left(Y; \overline{\beta}, \overline{y}_{pp}, P_{pp}\right) \delta_1[u] & \overline{\beta} \leq k^o - 1 \wedge \omega \geq k^o \\ \left(1 - p_1^{S,o}\right) p(Y)\, \delta_0[u] & \\ \quad + p_1^{S,o} \mathcal{N}\left(Y; \overline{\beta}, \overline{y}_{pn}, P_{pn}\right) \delta_1[u] & \omega = k^o - 1 \\ \left(1 - p_2^{S,o}\right) p(Y)\, \delta_0[u] & \\ \quad + p_2^{S,o} \mathcal{N}\left(Y; \overline{\beta}, \overline{y}_{np}, P_{np}\right) \delta_1[u] & \overline{\beta} = k^o \end{cases} \tag{35}$$

where $\omega = \overline{\beta} + \dim(\overline{x})/n_x - 1$ is the final time step. For $p(X)$ present at $k^o - 1$ and k^o, we have

$$\overline{y}_{pp} = \left[\overline{x}^T, (F_{pp}\overline{x})^T\right]^T,\ P_{pp} = \begin{bmatrix} P & PF_{pp}^T \\ F_{pp}P & F_{pp}PF_{pp}^T + Q_{pp} \end{bmatrix}$$

$$F_{pp} = \left[0_{n_x \times n_x\left(k^o-\overline{\beta}-1\right)}, F_1 - K_{pp}F_2F_1, K_{pp}, 0_{n_x \times n_x(\omega-k^o)}\right]$$

$$Q_{pp} = Q_1 - K_{pp}F_2Q_1 \tag{36}$$

$$K_{pp} = Q_1F_2^T\left(F_2Q_1F_2^T + Q_2\right)^{-1}. \tag{37}$$

For $p(X)$ present at k^o-1 but not at k^o, we have

$$\overline{y}_{pn} = \left[\overline{x}^T, (F_{pn}\overline{x})^T\right]^T,\ P_{pn} = \begin{bmatrix} P & PF_{pn}^T \\ F_{pn}P & F_{pn}PF_{pn}^T + Q_1 \end{bmatrix}$$

$$F_{pn} = \left[0_{n_x \times n_x(\omega-\overline{\beta})}, F_1\right].$$

For $p(X)$ not present at k^o-1 but present at k^o, we have

$$\overline{y}_{np} = \left[\overline{x}^T, ((I - K_{np}F_2)\,\overline{x}_{b,1} + F_{np}\overline{x})^T\right]^T$$

$$P_{np} = \begin{bmatrix} P & PF_{np}^T \\ F_{np}P & F_{np}PF_{np}^T + Q_{np} \end{bmatrix}$$

$$F_{np} = \left[K_{np}, 0_{n_x \times n_x\left(\omega-\overline{\beta}\right)}\right] \tag{38}$$

$$Q_{np} = P_{b,1} - K_{np}F_2P_{b,1} \tag{39}$$

$$K_{np} = P_{b,1}F_2^T\left(F_2P_{b,1}F_2^T + Q_2\right)^{-1}. \tag{40}$$

The proof of Lemma 5 is given in Appendix B. In the lemma, there is one entry per each of the entries in the transition density in Prop. 3. The first entry deals with trajectories that start after k^o or end before than k^o-1, which imply that there is no OOS state and the density remains unchanged. The second entry considers trajectories that are present at k^o-1 and k^o so the trajectory exists at the OOS time. The third entry correspond to trajectories that are present at k^o-1 but not at k^o, which implies that the trajectory is extended with probability $p_1^{S,o}$. The fourth entry represents trajectories not present at k^o-1 but present at k^o, in which case the trajectory is extended with probability $p_2^{S,o}$.

Applying Lemma 5 to each Gaussian component of the PPP (34) and the Bernoulli single-trajectory density in (33), we obtain the retrodicted PMBM density $f_{\tau,k|k}(\cdot)$, see (19) The number of components in the PPP and in (33) may increase due to the entries that have two terms in (35). After computing $f_{\tau,k|k}(\cdot)$, we apply the TPMBM update for a Gaussian implementation with all trajectories, explained in [26], [27], with some minor differences that are explained in Appendix C.

The marginalisation step for PMBMs on sets of trajectories is explained in [34]. In our case, this step marginalises out variable u and the state information corresponding to time τ for each Gaussian. The result is a Gaussian mixture of the form (33).

D. Implementation aspects

In this section, we discuss some aspects required for the implementation of the proposed OOS update. First of all, we implement the Gaussian CD-TPMBM for all trajectories in a similar manner as the TPMBM in [27]. That is, to deal with the high number of hypotheses, we use ellipsoidal gating for the data associations, Murty's algorithm to select global hypotheses with high weights, and pruning to remove global hypotheses and PPP components with low weights. If $\alpha_{k|k}^{i,a^i}(k)$ in (33) for a Bernoulli is less than a threshold Γ_a, we set $\alpha_{k|k}^{i,a^i}(k) = 0$, which implies that it is considered dead at time step k and is not further propagated through filtering.

The CD-TPMBM filter is implemented using an L-scan window. That is, for each single-trajectory density, the states corresponding to time steps outside the interval from $k-L+1$ to k are approximated as independent. This implies that the covariance matrices have a block-diagonal structure [27, Eq. (73)]. Due to this structure, in our implementation, we only process a set of OOS measurements if it arrives inside the L-scan window, i.e., $k^o \geq k-L+2$. Apart from the L-scan implementation, it is also possible to implement the Gaussian filters in information form [25], [26].

The CD-TPMB filter is analogous to the CD-TPMBM filter but adding a projection step after each update to keep the TPMB form [27]. Therefore, we can directly apply the proposed OOS update to a CD-TPMB filter followed by this projection step after the OOS measurement update.

VI. Simulations

In this section, we compare the CD-TPMBM and CD-TPMB filters, with and without OOS measurement processing[1]. The CD-TPMBM and CD-TPMB filters with the optimal OOS processing explained above are referred to as OOS-TPMBM and OOS-TPMB filters. If the OOS measurement time stamp is exactly the time stamp of an in-sequence measurement, we do not have to account for target appearances and disappearances at OOS time and proceed as in Sections IV and V. Instead, we can update each single trajectory density of the TPMBM filter using the approach in [4]. Therefore, we consider another baseline algorithm, in which for each OOS measurement, we calculate the nearest in-sequence measurement time stamp, and apply the single-trajectory update in [4]. We use the acronyms (N)OOS-TPMBM and (N)OOS-TPMB to refer to these variants of the filters. The variants of the filters without OOS measurement processing simply discard OOS measurements.

The filters have been implemented with the parameters: maximum number of global hypotheses $N_h = 200$, threshold for pruning global hypotheses 10^{-4}, threshold for PPP pruning $\Gamma_p = 10^{-5}$, $L \in \{3, 5\}$ and $\Gamma_a = 10^{-4}$. The TPMB filters estimate trajectories whose existence is higher than 0.5 [27, Sec. V.D] and the TPMBM filters use Estimator 1 in [29] with threshold 0.4. The algorithms are implemented in Matlab with the compiled Murty's algorithm in [39].

We consider a 2-D scenario with the Wiener velocity model and dynamic parameters: $\lambda = 0.12\,\mathrm{s}^{-1}$, $\mu = 0.02\,\mathrm{s}^{-1}$, $q = 0.2\,\mathrm{m}^2/\mathrm{s}^3$, $d = 2$. Thus, the average life span of a target is $1/\mu = 50\,\mathrm{s}$ and, in the stationary regime of the birth/death process, the number of alive targets is Poisson distributed with parameter $\frac{\lambda}{\mu} = 6$. The prior moments at appearance time are: $\overline{x}_a = \left[\overline{p}_a^T, \overline{v}_a^T\right]^T$ with $\overline{p}_a = [200, 200]^T\,(\mathrm{m})$,

[1]Matlab code is available at https://github.com/Agarciafernandez/MTT.

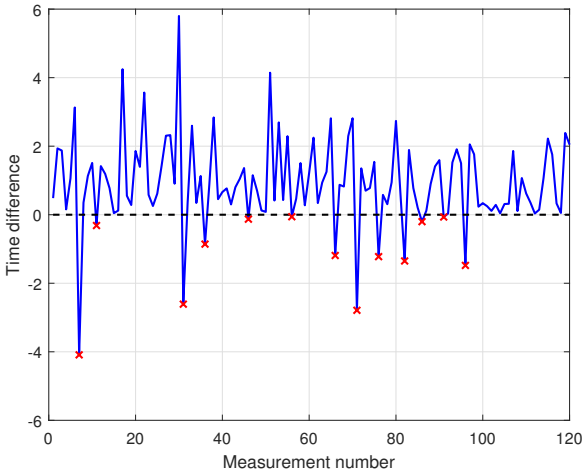

Figure 4: Time difference between received measurements. OOS measurements have a negative time difference and are highlighted with a red cross.

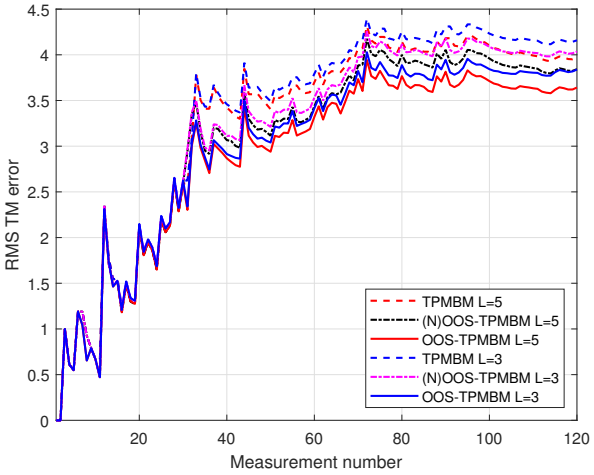

Figure 6: RMS trajectory metric error to estimate the set of all trajectories for each received measurement. The TPMBM filter with optimal OOS processing with $L = 5$ has the lowest error.

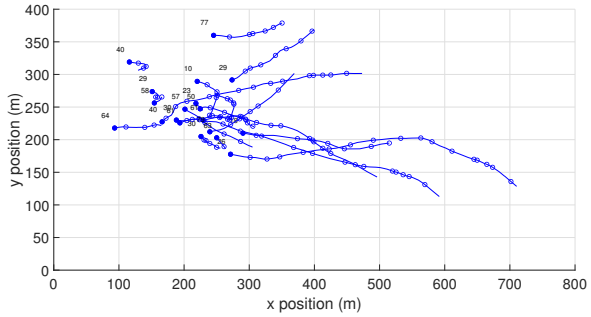

Figure 5: Scenario of the simulations with the set of trajectories sampled at the in-sequence measurement time steps. The beginning of a trajectory is marked with a filled circle and its position every 10 time steps is marked with a circle. A number next to the trajectory start time indicates the (in-sequence) time step when it was born.

$\overline{v}_a = [3, 0]^T$ (m/s), and $P_a = \text{diag}([P_a^{pp}, P_a^{vv}])$ with $P_a^{pp} = \text{diag}([50^2, 50^2])$ (m^2) and $P_a^{vv} = \text{diag}([1, 1])$ (m^2/s^2).

The sensor measures position with likelihood $l(\cdot|x) = \mathcal{N}(\cdot; Hx, R)$,

$$H = \begin{pmatrix} 1 & 0 & 0 & 0 \\ 0 & 1 & 0 & 0 \end{pmatrix}, \quad R = \sigma^2 I_2,$$

where $\sigma^2 = 4\,(\text{m}^2)$, and $p_D = 0.9$. The clutter intensity is $\lambda^C(z) = \overline{\lambda}^C u_A(z)$ where $u_A(\cdot)$ is a uniform density in $A = [0, 800] \times [0, 400]$ (m) and $\overline{\lambda}^C = 10$. The sensor takes 120 measurements with a time interval between measurements that is drawn from an exponential distribution with parameter $\mu_m = 1\,\text{s}^{-1}$. To simulate OOS measurements, for every 5 of the 120 measurements, we draw a random number n_o from a Poisson distribution with parameter 1 and place this measurement n_o time steps afterwards. The resulting time difference between received measurements in our simulation is shown in Figure 4.

The scenario of the simulations is shown in Figure 5. There are 19 targets in total and the maximum number of targets alive at the same time step is 10. We evaluate the filters via Monte Carlo simulation with $N_{mc} = 100$ runs. For each received measurement and Monte Carlo run i, we calculate the error between the true set $\mathbf{X}_k$ of all trajectories up to the current time and its estimate $\hat{\mathbf{X}}_k^i$ (both sampled at in-sequence sampling times). The error is calculated by the metric $d(\cdot,\cdot)$ for sets of trajectories in [40] with parameters $p = 2$, $c = 10$ and $\gamma = 1$. We only use the position elements of the trajectories to compute $d(\cdot,\cdot)$ and normalise the squared error by the length of the time window to obtain $d^2\left(\mathbf{X}_k, \hat{\mathbf{X}}_k^i\right)/k$. The root mean square (RMS) error at time step k is

$$d(k) = \sqrt{\frac{1}{N_{mc}k}\sum_{i=1}^{N_{mc}} d^2\left(\mathbf{X}_k, \hat{\mathbf{X}}_k^i\right)}. \tag{41}$$

The RMS trajectory metric (TM) errors (41) of the TPMBM algorithms against the measurement number are shown in Figure 6. As expected, for a given L, the OOS-TPMBM filter is the one with lowest error, followed by the (N)OOS-TPMBM filter, and the TPMBM filter without OOS processing. The filters with $L = 5$ have lower error than the filters with $L = 3$, as they update a longer time window. We can also see that all filters have quite similar performance up to around processing 30 measurements, when differences arise. The reason is that for the first two OOS measurement, see Figure 4, there are not any targets present yet, and the processing of the OOS measurements does not improve performance. It is the processing of the subsequent OOS measurement that have an impact on performance.

To analyse more thoroughly filter performance, we show the decomposition of the trajectory metric in Figure 7. The filters without OOS processing have a higher false target cost. The main reason is that the start time of a trajectory (the one born at at time step 29 with position $[151, 174]^T$ (m)) is estimated more accurately by processing the third OOS measurement. The filters with optimal OOS processing show better performance than (N)OOS processing mainly due to improvement in localisation cost. Increasing L decreases the localisation costs,

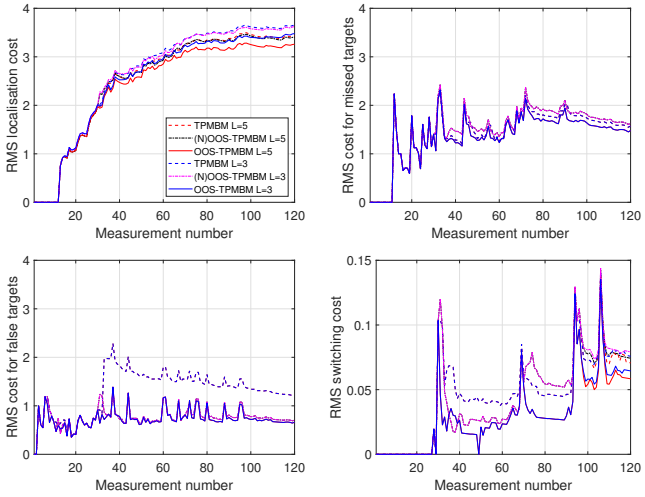

Figure 7: RMS trajectory metric decomposition into localisation cost, missed target cost, false target cost and track switching cost for each received measurement. Filters with OOS measurement processing mainly lower the cost for false targets in this scenario.

Table II: RMS trajectory metric and its decomposition across all time steps, and computational time in seconds

L	Algorithm	Tot.	Loc.	Fal.	Mis.	Swi.	Time
5	TPMBM	3.44	2.76	1.37	1.52	0.06	11.3
	(N)OOS-TPMBM	3.28	2.75	0.79	1.59	0.05	11.9
	OOS-TPMBM	3.10	2.63	0.75	1.46	0.04	12.3
	TPMB	3.84	2.77	1.39	2.28	0.07	2.5
	(N)OOS-TPMB	3.51	2.71	0.86	2.05	0.07	3.0
	OOS-TPMB	3.42	2.63	0.78	2.04	0.05	3.0
3	TPMBM	3.54	2.88	1.37	1.52	0.06	11.0
	(N)OOS-TPMBM	3.37	2.87	0.79	1.59	0.06	11.8
	OOS-TPMBM	3.20	2.74	0.75	1.46	0.04	12.3
	TPMB	3.93	2.88	1.40	2.28	0.07	2.5
	(N)OOS-TPMB	3.61	2.83	0.87	2.05	0.07	3.0
	OOS-TPMB	3.52	2.75	0.79	2.05	0.06	3.0

as the filters are able to improve estimation of past states. Track switching costs are zero up to measurement number 26.

In Table II, we show the RMS trajectory metric error across all time steps [27], also including TPMB filter performance and the average time to run one Monte Carlo iteration of our implementations with a 1.6 GHz Intel i5 laptop. As indicated before, the best performing filter is the OOS-TPMBM with $L = 5$. In this scenario, the TPMB approximation mainly implies an increase in the number of missed targets, irrespective of the type of OOS processing. As expected, processing OOS measurements increases running times. TPMBM filters have higher computational complexity than TPMB filters. There is little difference in computational times between $L = 3$ and $L = 5$.

VII. Conclusions

This paper has explained how to perform the Bayesian update with out-of-sequence measurements for multiple target tracking when the multi-target dynamics are given in continuous time and we compute the posterior of the set of all sampled trajectories. When processing in-sequence measurements, the posterior density of the set of all sampled trajectories is a Poisson multi-Bernoulli mixture. This paper shows that the processing of out-of-sequence measurements consists of two steps: retrodiction and update. After performing these two steps, the posterior is also a Poisson multi-Bernoulli mixture.

The paper also explains the out-of-sequence measurement processing when we consider a Gaussian implementation of the trajectory Poisson multi-Bernoulli mixture filter. Simulation results show that lower error is achieved by optimally processing out-of-sequence measurements.

References

[1] S. Challa, M. R. Morelande, D. Musicki, and R. J. Evans, *Fundamentals of Object Tracking*. Cambridge University Press, 2011.

[2] X. R. Li and Y. Bar-Shalom, "Design of an interacting multiple model algorithm for air traffic control tracking," *IEEE Transactions on Control Systems Technology*, vol. 1, no. 3, pp. 186–194, Sep. 1993.

[3] B. Fortin, R. Lherbier, and J. Noyer, "A model-based joint detection and tracking approach for multi-vehicle tracking with lidar sensor," *IEEE Transactions on Intelligent Transportation Systems*, vol. 16, no. 4, pp. 1883–1895, 2015.

[4] W. Koch and F. Govaers, "On accumulated state densities with applications to out-of-sequence measurement processing," *IEEE Transactions on Aerospace and Electronic Systems*, vol. 47, no. 4, pp. 2766–2778, 2011.

[5] Y. Bar-Shalom, "Update with out-of-sequence measurements in tracking: exact solution," *IEEE Transactions on Aerospace and Electronic Systems*, vol. 38, no. 3, pp. 769–777, Jul. 2002.

[6] Y. Bar-Shalom, H. Chen, and M. Mallick, "One-step solution for the multistep out-of-sequence-measurement problem in tracking," *IEEE Transactions on Aerospace and Electronic Systems*, vol. 40, no. 1, pp. 27–37, 2004.

[7] K. Zhang, X. R. Li, and Y. Zhu, "Optimal update with out-of-sequence measurements," *IEEE Transactions on Signal Processing*, vol. 53, no. 6, pp. 1992–2004, June 2005.

[8] S. Zhang and Y. Bar-Shalom, "Out-of-sequence measurement processing for particle filter: Exact Bayesian solution," *IEEE Transactions on Aerospace and Electronic Systems*, vol. 48, no. 4, pp. 2818–2831, Oct. 2012.

[9] M. Orton and A. Marrs, "Particle filters for tracking with out-of-sequence measurements," *IEEE Transactions on Aerospace and Electronic Systems*, vol. 41, no. 2, pp. 693–702, April 2005.

[10] F. Govaers and W. Koch, "Generalized solution to smoothing and out-of-sequence processing," *IEEE Transactions on Aerospace and Electronic Systems*, vol. 50, no. 3, pp. 1739–1748, July 2014.

[11] X. Shen, Y. Zhu, E. Song, and Y. Luo, "Optimal centralized update with multiple local out-of-sequence measurements," *IEEE Transactions on Signal Processing*, vol. 57, no. 4, pp. 1551–1562, 2009.

[12] M. Orton and A. Marrs, "A Bayesian approach to multi-target tracking and data fusion with out-of-sequence measurements," in *IEE Target Tracking: Algorithms and Applications*, 2001, pp. 15/1–15/5 vol.1.

[13] K. Zhang, X. Li, H. Chen, and M. Mallick, "Multi-sensor multi-target tracking with out-of-sequence measurements," in *Proceedings of the Sixth International Conference of Information Fusion*, vol. 1, 2003, pp. 672–679.

[14] S. Maskell, R. G. Everitt, R. Wright, and M. Briers, "Multi-target out-of-sequence data association: Tracking using graphical models," *Information Fusion*, vol. 7, no. 4, pp. 434 – 447, 2006.

[15] M. Mallick, J. Krant, and Y. Bar-Shalom, "Multi-sensor multi-target tracking using out-of-sequence measurements," in *Proceedings of the Fifth International Conference on Information Fusion*, vol. 1, 2002, pp. 135–142.

[16] S. Chan and R. Paffenroth, "Out-of-sequence measurement updates for multi-hypothesis tracking algorithms," in *Proceedings SPIE Signal and Data Processing of Small Targets*, vol. 6969, pp. 1–12.

[17] Q. Yang and W. Yi, "An efficient PHD filter for multi-target tracking with out-of-sequence measurement," in *IEEE Radar Conference*, 2020, pp. 1–6.

[18] A. F. García-Fernández and S. Maskell, "Continuous-discrete multiple target filtering: PMBM, PHD and CPHD filter implementations," *IEEE Transactions on Signal Processing*, vol. 68, pp. 1300–1314, 2020.

[19] S. Coraluppi and C. A. Carthel, "If a tree falls in the woods, it does make a sound: multiple-hypothesis tracking with undetected target births," *IEEE Transactions on Aerospace and Electronic Systems*, vol. 50, no. 3, pp. 2379–2388, July 2014.

[20] A. F. García-Fernández and S. Maskell, "Continuous-discrete trajectory PHD and CPHD filters," in *23rd International Conference on Information Fusion*, 2020, pp. 1–8.

[21] L. Kleinrock, *Queueing Systems*. John Wiley & Sons, 1976.

[22] S. Särkkä and A. Solin, *Applied Stochastic Differential Equations*. Cambridge University Press, 2019.

[23] R. P. S. Mahler, *Advances in Statistical Multisource-Multitarget Information Fusion*. Artech House, 2014.

[24] A. F. García-Fernández, L. Svensson, and M. R. Morelande, "Multiple target tracking based on sets of trajectories," *IEEE Transactions on Aerospace and Electronic Systems*, vol. 56, no. 3, pp. 1685–1707, Jun. 2020.

[25] K. Granström, L. Svensson, Y. Xia, J. L. Williams, and A. F. García-Fernández, "Poisson multi-Bernoulli mixture trackers: continuity through random finite sets of trajectories," in *21st International Conference on Information Fusion*, 2018, pp. 973–981.

[26] K. Granström, L. Svensson, Y. Xia, J. Williams, and A. F. García-Fernández, "Poisson multi-Bernoulli mixtures for sets of trajectories," 2019. [Online]. Available: https://arxiv.org/abs/1912.08718

[27] A. F. García-Fernández, L. Svensson, J. L. Williams, Y. Xia, and K. Granström, "Trajectory Poisson multi-Bernoulli filters," *IEEE Transactions on Signal Processing*, vol. 68, pp. 4933–4945, 2020.

[28] J. L. Williams, "Marginal multi-Bernoulli filters: RFS derivation of MHT, JIPDA and association-based MeMBer," *IEEE Transactions on Aerospace and Electronic Systems*, vol. 51, no. 3, pp. 1664–1687, July 2015.

[29] A. F. García-Fernández, J. L. Williams, K. Granström, and L. Svensson, "Poisson multi-Bernoulli mixture filter: direct derivation and implementation," *IEEE Transactions on Aerospace and Electronic Systems*, vol. 54, no. 4, pp. 1883–1901, Aug. 2018.

[30] D. Reid, "An algorithm for tracking multiple targets," *IEEE Transactions on Automatic Control*, vol. 24, no. 6, pp. 843–854, Dec. 1979.

[31] E. F. Brekke and M. Chitre, "The multiple hypothesis tracker derived from finite set statistics," in *20th International Conference on Information Fusion*, 2017, pp. 1–8.

[32] E. Brekke and M. Chitre, "Relationship between finite set statistics and the multiple hypothesis tracker," *IEEE Transactions on Aerospace and Electronic Systems*, vol. 54, no. 4, pp. 1902–1917, Aug. 2018.

[33] P. Boström-Rost, D. Axehill, and G. Hendeby, "Sensor management for search and track using the Poisson multi-Bernoulli mixture filter," *IEEE Transactions on Aerospace and Electronic Systems*, 2021.

[34] K. Granström, L. Svensson, Y. Xia, A. F. García-Fernández, and J. L. Williams, "Spatiotemporal constraints for sets of trajectories with applications to PMBM densities," in *23rd International Conference on Information Fusion*, 2020, pp. 1–8.

[35] M. Fröhle, K. Granström, and H. Wymeersch, "Decentralized Poisson multi-Bernoulli filtering for vehicle tracking," *IEEE Access*, vol. 8, pp. 126 414–126 427, 2020.

[36] V. G. Kulkarni, *Modeling and analysis of stochastic systems*. Chapman & Hall/CRC, 2016.

[37] Y. Xia, K. Granström, L. Svensson, A. F. García-Fernández, and J. L. Wlliams, "Multi-scan implementation of the trajectory Poisson multi-Bernoulli mixture filter," *Journal of Advances in Information Fusion*, vol. 14, no. 2, pp. 213–235, Dec. 2019.

[38] R. Streit, *Poisson point processes: Imaging, tracking, and sensing*. Springer, 2010.

[39] D. F. Crouse, "The tracker component library: free routines for rapid prototyping," *IEEE Aerospace and Electronic Systems Magazine*, vol. 32, no. 5, pp. 18–27, 2017.

[40] A. F. García-Fernández, A. S. Rahmathullah, and L. Svensson, "A metric on the space of finite sets of trajectories for evaluation of multi-target tracking algorithms," *IEEE Transactions on Signal Processing*, vol. 68, pp. 3917–3928, 2020.

[41] S. N. Chiu, D. Stoyan, W. S. Kendall, and J. Mecke, *Stochastic Geometry and its Applications*. John Wiley & Sons, 2013.

[42] A. F. García-Fernández and L. Svensson, "Trajectory PHD and CPHD filters," *IEEE Transactions on Signal Processing*, vol. 67, no. 22, pp. 5702–5714, Nov 2019.

[43] S. Särkkä, *Bayesian Filtering and Smoothing*. Cambridge University Press, 2013.

Continuous-discrete multiple target tracking with out-of-sequence measurements: Supplementary material

APPENDIX A

In this appendix, we explain how to calculate $p_1^{S,o}$ and $p_2^{S,o}$ in Proposition 3, and also provide the proof of Theorem 4.

A. Probability $p_1^{S,o}$

The probability $p_1^{S,o}$ corresponds to the probability that a trajectory that is alive at time step k^o-1, but not at k^o, is alive at time τ. In this subsection, we denote the time lag of disappearance of this trajectory w.r.t. t_{k^o-1} as t, which implies that the trajectory disappears at time $t+t_{k^o-1}$. Given that the trajectory is alive at time step k^o-1, the distribution of the time lag of disappearance is an exponential distribution with parameter μ [18]. Then, given that the trajectory is alive at time step k^o-1 and dead at time step k^o, the distribution of t is a truncated exponential distribution

$$p_k^o(t) = \frac{\mu}{1-e^{-\mu\Delta t_{k^o}}} e^{-\mu t} \chi_{[0,\Delta t_{k^o})}(t). \tag{42}$$

Therefore, the probability that this trajectory is alive at time τ is the probability that $t \geq \Delta t_{o,1}$ (i.e. it disappears after time τ), which is calculated as

$$p_1^{S,o} = \int_{\Delta t_{o,1}}^{\Delta t_{k^o}} p_k^o(t)\, dt = p_k^{S,o}(\Delta t_{o,1}) \tag{43}$$

where $p_k^{S,o}(\cdot)$ is given by (16).

B. Probability $p_2^{S,o}$

The probability $p_2^{S,o}$ corresponds to the probability that a trajectory that is not alive at time step k^o-1, but it is at k^o, is alive at time τ. This implies that this trajectory is born at time step k^o and has appeared between times t_{k^o-1} and t_{k^o}. In this section, we denote the time lag of appearance w.r.t. t_{k^o} as t, which implies that the trajectory appears at time $t_{k^o}-t$. The distribution of t is the truncated exponential distribution (42) [18]. Then, the probability that the trajectory is alive at time τ is the probability that $t \geq \Delta t_{o,2}$ (i.e. it appears before time τ), which can be calculated as

$$p_2^{S,o} = \int_{\Delta t_{o,2}}^{\Delta t_{k^o}} p_k^o(t)\, dt = p_k^{S,o}(\Delta t_{o,2}). \tag{44}$$

C. Proof of Theorem 4

We prove Theorem 4 by noticing that the retrodiction step corresponds to a PMBM prediction step with a suitable choice of single-object transition density and PPP intensity for new born objects [25], [28].

We first obtain the intensity for the set of OOS new trajectories $\mathbf{N}$. The trajectories in $\mathbf{N}$ existed at time step τ, and appeared and disappeared between time steps k^o-1 and k^o. That is, these trajectories appeared in an interval $\Delta t_{o,1}$ and are alive at its end, and disappeared in the following time interval $\Delta t_{o,2}$. Due to the continuous time multi-target model and the independent increments property of PPPs [23, pp. 99], $\mathbf{N}$ is independent of the sampled set of trajectories $\mathbf{X}_k$. In addition, $\mathbf{N}$ corresponds to a thinning operation on a birth PPP with intensity (7) (on an interval $\Delta t_{o,1}$ instead of Δt_k). This thinning operation produces a PPP $\lambda^B_{\tau,k|k}(\cdot)$ with the same spatial distribution [41]. Also, the expected number $w^B(\Delta t_{o,1}, \Delta t_{o,2})$ of OOS new trajectories, which is the integral of $\lambda^B_{\tau,k|k}(\cdot)$, is the expected number of trajectories that appear in an interval $\Delta t_{o,1}$ and are alive at its end, which is given by $\frac{\lambda}{\mu}\left(1-e^{-\mu\Delta t_{o,1}}\right)$ [18], [36], multiplied by the probability that a trajectory disappears in an interval $\Delta t_{o,2}$, which is given by $\left(1-e^{-\mu\Delta t_{o,2}}\right)$, see (3). We then obtain the intensity in (23) by adding the information that the trajectories have length one with a single state at time τ, and are marked with $\beta=-1$.

Each $X \in \mathbf{X}_k$ is transformed with probability one to $(u, Y) \in \mathbf{X}_k^{\mathrm{a}}$ and transition density $g_{\tau,k|k}(u, Y|X)$ in Proposition 3. With these results, we can now apply the PMBM prediction step [25], [28], [29] to obtain the density of $\mathbf{Y}_k = \mathbf{X}_k^{\mathrm{a}} \cup \mathbf{N}$, which yields Theorem 4.

APPENDIX B

In this appendix, we prove Lemma 5. In this lemma, we should first note that $p(X)$ represents a trajectory with known start time $\overline{\beta}$ and end time ω, so the trajectory integral (1) reduces to a standard integral on an Euclidean space. The first entry in (35) is the integral w.r.t. a Dirac delta on the single-trajectory space, which leaves the density $p(\cdot)$ unchanged, evaluated at Y. The third entry corresponds to the transition density applied to a density that is present at time step k^o-1 but not at k^o. The output has two terms. The first one is the integral w.r.t. a Dirac delta that leaves $p(\cdot)$ unchanged. The second term is straightforward as the transition density is a linear/Gaussian dynamic model with transition matrix F_1 and covariance matrix Q_1, which is extended to include full trajectory information, see also [27], [42]. The second and fourth entries in (35) are more complicated, so we analyse them in the next subsections.

A. Trajectory present at k^o-1 and k^o

The second entry corresponds to the transition density applied to a density of a trajectory that is present at both time steps k^o-1 and k^o. We proceed to calculate the corresponding transition density (17) for the Wiener velocity model. For notational simplicity, we denote x_1 and x_2 the states of $\left(\overline{\beta}, x^{1:i}\right)$ at steps k^o-1 and k^o. Then, (17) is analogous to the Kalman filter update of a prior

$$\mathcal{N}(y; F_1 x_1, Q_1)$$

with a measurement density (on x_2)

$$\mathcal{N}(x_2; F_2 y, Q_2).$$

By direct application of the Kalman filter update [43], we obtain

$$p(y|x_1,x_2) = \mathcal{N}\left(y; [F_1 - K_{pp}F_2F_1,\ K_{pp}] \begin{bmatrix} x_1 \\ x_2 \end{bmatrix}, Q_{pp}\right) \tag{45}$$

where K_{pp} and Q_{pp} are defined in Lemma 5. Then, the integral of Lemma 5 corresponds to the density of a Gaussian density augmented with another state y whose conditional density is Gaussian. The result is a Gaussian with moments in Lemma 5. Note that in the lemma we write the transition matrix F_{pp} applied to the whole trajectory, not only to x_1 and x_2.

B. Trajectory present at k^o but not at $k^o - 1$

The fourth entry corresponds to the transition density applied to a density of a trajectory that is present at time step k^o but not at $k^o - 1$. There are two terms in the output. The first one corresponds to the Dirac delta and leaves the density $p(\cdot)$ unaltered. It represents that the trajectory appeared at a time between τ and t_{k^o}. The second term considers the hypothesis that the trajectory appeared at a time between t_{k^o-1} and time τ, and is therefore alive at time τ and at time step t_{k^o}. We proceed to compute this term by first calculating the transition density (18) for the Wiener velocity model.

The integral w.r.t. t in (18) is approximated by the Gaussian that minimises the KLD. Its mean and covariance are denoted by $\overline{x}_{b,1}$ and $P_{b,1}$ and are given by Prop. 2 in [18] using $\Delta t_{o,1}$ as the time interval. After this approximation, the transition density $p\left(y|x^1\right)$ can be calculated as the Kalman filter update of a prior with moments $\overline{x}_{b,1}$ and $P_{b,1}$ and a measurement density (on x^1)

$$\mathcal{N}\left(x^1; F_2 y, Q_2\right). \tag{46}$$

This yields

$$p\left(y|x^1\right) = \mathcal{N}\left(y; \left(I - K_{np}F_2\right)\overline{x}_{b,1} + K_{np}x^1, Q_{np}\right), \tag{47}$$

where K_{np} and Q_{np} are given in Lemma 5. Then, as in Section B-A, the output of the integral is Gaussian with the moments in Lemma 5.

APPENDIX C

In this appendix, we provide more details on the TPMBM Gaussian update [25], [27] with OOS measurements. In particular, we provide the steps on how to compute the updated local hypotheses for previous Bernoulli components, which is the main difficulty in the update.

In the standard TPMBM Gaussian update for in-sequence measurements, there is only one hypothesis (term in the mixture) of each Bernoulli, see (33) and [27, Eq. (64)], that has information on the current state of the trajectory. On the contrary, for OOS measurement processing, there may be more than one term that has information on the state at OOS measurement time due to the application of Lemma 5 to each Gaussian in (33).

We write the retrodicted single-target density for previous Bernoulli i with local hypothesis a^i as

$$\begin{aligned}
&p^{i,a^i}_{\tau,k|k}(u,Y) \\
&= \delta_0[u] \sum_{\kappa=\beta^{i,a^i}}^{k} \alpha^{i,a^i}_{0,k|k}(\kappa)\mathcal{N}\left(Y; \beta^{i,a^i}, \overline{x}^{i,a^i}_{k|k}(\kappa), P^{i,a^i}_{k|k}(\kappa)\right) \\
&+ \delta_1[u] \sum_{\kappa=\beta^{i,a^i}}^{k} \alpha^{i,a^i}_{1,k|k}(\kappa)\mathcal{N}\left(Y; \beta^{i,a^i}, \overline{x}^{i,a^i}_{\tau,k|k}(\kappa), P^{i,a^i}_{\tau,k|k}(\kappa)\right)
\end{aligned} \tag{48}$$

where

$$\alpha^{i,a^i}_{0,k|k}(\kappa) = \alpha^{i,a^i}_{k|k}(\kappa)\left(1 - p(\kappa)\right) \tag{49}$$

$$\alpha^{i,a^i}_{1,k|k}(\kappa) = \alpha^{i,a^i}_{k|k}(\kappa)\, p(\kappa) \tag{50}$$

where $p(\kappa) \in \left\{0, 1, p_1^{S,o}, p_2^{S,o}\right\}$ depending on the corresponding entry of Lemma 5 for each Gaussian in (33). The Gaussian components that are augmented with an OOS state have $u = 1$, mean and covariances $\overline{x}^{i,a^i}_{\tau,k|k}(\kappa)$ and $P^{i,a^i}_{\tau,k|k}(\kappa)$, and are included in the third line in (48). The Gaussian components without state augmentation have $u = 0$, remain unchanged w.r.t. the prior, and are included in the second line in (48).

In the rest of the appendix, Sections C-A and C-B explain the update with a misdetection and a detection, respectively.

A. Misdetection hypothesis

The update with misdetection hypothesis of a Bernoulli with single-trajectory density (48) is

$$\begin{aligned}
&p^{i,a^i}_{\tau,k|\tau,k}(u,Y) \\
&\propto \delta_0[u] \sum_{\kappa=\beta^{i,a^i}}^{k} \alpha^{i,a^i}_{0,k|k}(\kappa)\mathcal{N}\left(Y; \beta^{i,a^i}, \overline{x}^{i,a^i}_{k|k}(\kappa), P^{i,a^i}_{k|k}(\kappa)\right) \\
&+ \delta_1[u] \sum_{\kappa=\beta^{i,a^i}}^{k} \alpha^{i,a^i}_{1,k|\tau,k}(\kappa)\mathcal{N}\left(Y; \beta^{i,a^i}, \overline{x}^{i,a^i}_{\tau,k|k}(\kappa), P^{i,a^i}_{\tau,k|k}(\kappa)\right)
\end{aligned} \tag{51}$$

where, in this case,

$$\alpha^{i,a^i}_{1,k|\tau,k}(\kappa) = \left(1 - p^D\right)\alpha^{i,a^i}_{1,k|k}(\kappa). \tag{52}$$

We can see that the Gaussian densities in (51) are unchanged after the update. The update only changes the weights of terms with an OOS state by multiplying them by $\left(1 - p^D\right)$, see (52).

The weight and existence probability of the updated Bernoulli with local hypothesis a^i become [25], [28]

$$w^{i,a^i}_{\tau,k|\tau,k} = w^{i,a^i}_{k|k}\left(1 - r^{i,a^i}_{k|k} p^D \sum_{\kappa=\beta^{i,a^i}}^{k} \alpha^{i,a^i}_{1,k|k}(\kappa)\right) \tag{53}$$

$$r^{i,a^i}_{\tau,k|\tau,k} = \frac{r^{i,a^i}_{k|k}\left(1 - p^D \sum_{\kappa=\beta^{i,a^i}}^{k} \alpha^{i,a^i}_{1,k|k}(\kappa)\right)}{1 - r^{i,a^i}_{k|k} p^D \sum_{\kappa=\beta^{i,a^i}}^{k} \alpha^{i,a^i}_{1,k|k}(\kappa)}. \tag{54}$$

It should be noted that $p^D \sum_{\kappa=\beta^{i,a^i}}^{k} \alpha^{i,a^i}_{1,k|k}(\kappa)$ is the average probability of detection at OOS time for a prior (48).

B. Detection hypothesis

The update of a Bernoulli with a single-trajectory density (48) with a measurement z (corresponding to an updated local hypothesis $\widetilde{a}^i$) is [28]

$$p^{i,\widetilde{a}^i}_{\tau,k|\tau,k}(u,Y) \propto \delta_1[u] \sum_{\kappa=\beta^{i,a^i}}^{k} \alpha^{i,\widetilde{a}^i}_{1,k|\tau,k}(\kappa)$$

$$\times \mathcal{N}\left(Y;\beta^{i,a^i},\overline{x}^{i,\widetilde{a}^i}_{\tau,k|\tau,k}(\kappa),P^{i,\widetilde{a}^i}_{\tau,k|\tau,k}(\kappa)\right) \tag{55}$$

where $\overline{x}^{i,\widetilde{a}^i}_{\tau,k|\tau,k}(\kappa)$ and $P^{i,\widetilde{a}^i}_{\tau,k|\tau,k}(\kappa)$ are obtained by a Kalman filter update on a Gaussian single-trajectory prior with mean $\overline{x}^{i,a^i}_{\tau,k|k}(\kappa)$ and covariance $P^{i,a^i}_{\tau,k|k}(\kappa)$, see (53)-(57) in [27]. In addition, the weights of the mixture in (55) are

$$\alpha^{i,\widetilde{a}^i}_{1,k|\tau,k}(\kappa) = p^D \mathcal{N}\left(z;\overline{z}^{i,a^i}(\kappa),S^{i,a^i}(\kappa)\right)\alpha^{i,a^i}_{1,k|k}(\kappa) \tag{56}$$

where $\overline{z}^{i,a^i}(\kappa)$ and $S^{i,a^i}(\kappa)$ are the mean and covariance matrix of the predicted measurement for hypothesis κ [27].

The weight and existence probability of the updated Bernoulli with local hypothesis $\widetilde{a}^i$ are

$$w^{i,\widetilde{a}^i}_{\tau,k|\tau,k} = w^{i,a^i}_{k|k} r^{i,a^i}_{k|k} \sum_{\kappa=\beta^{i,a^i}}^{k} \alpha^{i,a^i}_{1,k|\tau,k}(\kappa) \tag{57}$$

$$r^{i,\widetilde{a}^i}_{\tau,k|\tau,k} = 1. \tag{58}$$

As this is a detection hypothesis, we have that the updated probability $r^{i,\widetilde{a}^i}_{\tau,k|\tau,k}$ of existence is 1. Moreover, the Gaussian components with factor $\delta_0[u]$ in the prior (48) cannot be detected, as they do not exist at OOS time, so they do not appear in the posterior (55). Then, the posterior weight $\alpha^{i,\widetilde{a}^i}_{1,k|\tau,k}(\kappa)$, see (56), depends on its previous weight $\alpha^{i,a^i}_{1,k|k}(\kappa)$ and how well this component explains the received measurement.